European Journal of Medicinal Chemistry 126 (2017) 110–121

Contents lists available at ScienceDirect

European Journal of Medicinal Chemistry

journal homepage: http://www.elsevier.com/locate/ejmech

Research paper

Synthesis, spectroscopic properties and photodynamic activity of two cationic BODIPY derivatives with application in the photoinactivation of microorganisms

Maximiliano L. Agazzi [1], M. Belén Ballatore [1], Eugenia Reynoso, Ezequiel D. Quiroga, Edgardo N. Durantini*

Departamento de Química, Facultad de Ciencias Exactas, Físico-Químicas y Naturales, Universidad Nacional de Río Cuarto, Ruta Nacional 36 Km 601, X5804BYA Río Cuarto, Córdoba, Argentina

ARTICLE INFO

Article history:
Received 23 August 2016
Received in revised form
19 September 2016
Accepted 1 October 2016
Available online 3 October 2016

Keywords:
BODIPY
Photosensitizer
Photooxidation
Singlet oxygen
Potassium iodide
Photodynamic inactivation

ABSTRACT

Two cationic BODIPYs **3** and **4** were synthesized by acid-catalyzed condensation of the corresponding pyrrole and benzaldehyde, followed by complexation with boron and methylation. Compound **3** contains methyl at the 1,3,5 and 7 positions of the *s*-indacene ring and a *N*,*N*,*N*-trimethylamino group attached to the phenylene unit, while **4** is not substituted by methyl groups and the cationic group is bound by an aliphatic spacer. UV-visible absorption spectra of these BODIPYs show an intense band at ~500 nm in solvents of different polarities and *n*-heptane/sodium bis(2-ethylhexyl)sulfosuccinate (AOT)/water reverse micelles. Compound **3** exhibits a higher fluorescence quantum yield (Φ_F = 0.29) than **4** (Φ_F = 0.030) in *N*,*N*-dimethylformamide (DMF) due to sterically hindered rotation of the phenylene ring. BODIPYs **3** and **4** induce photosensitized oxidation of 1,3-diphenylisobenzofuran (DPBF) with yields of singlet molecular oxygen of 0.07 and 0.03, respectively. However, the photodynamic activity increases in a microheterogenic medium formed by AOT micelles. Also, both BODIPYs sensitize the photodecomposition of L-tryptophan (Trp). In presence of diazabicyclo[2.2.2]octane (DABCO) or D-mannitol, a reduction in the photooxidation of Trp was found, indicating a contribution of type I photoprocess. Moreover, the addition of KI produces fluorescence quenching of BODIPYs and reduces the photooxidation of DPBF. In contrast, this inorganic salt increases the photoinduced decomposition of Trp, possibly due to the formation of reactive iodine species. The effect of KI was also observed in the potentiation of the photoinactivation of microorganisms. Therefore, the presence of KI could increase the decomposition of biomolecules induced by these BODIPYs in a biological media, leading to a higher cell photoinactivation.

1. Introduction

Infectious diseases may become non curable owing to high levels of multiple drug resistant pathogens [1]. The best epidemiologically documented resistance with high clinical impact includes the Gram-positive pathogen *Staphylococcus aureus* [2]. In this context, the Gram-negative organism *Escherichia coli*, not only causes severe hospital-acquired infections but also has an important reservoir in animals and the environment. Moreover, the clinical outcome of a systemic fungal infection is a very difficult task and the antifungal drug resistance is one of factors contributing to therapeutic failure [3]. In particular, antifungal drug resistance is just one of many factors contributing to therapeutic failure in *Candida albicans*. Therefore, microbial resistance against antibiotics is a serious global health issue and it has posed new challenge to researchers [1]. Photodynamic inactivation (PDI) has been proposed as an interesting approach to eradication of microorganisms [4]. PDI involves the addition of a photosensitizer that is rapidly bound to cells. The irradiation of the infection with visible light in presence of oxygen produces highly reactive oxygen species (ROS), which react with biomolecules of cellular environment. These processes induce a loss of biological functionality leading to cell inactivation [5]. In PDI, two mechanisms can be mainly involved

* Corresponding author.
E-mail address: edurantini@exa.unrc.edu.ar (E.N. Durantini).
[1] These authors contributed equally to this work.

http://dx.doi.org/10.1016/j.ejmech.2016.10.001
0223-5234/

after activation of the photosensitizer [6]. In the type I pathway, the photosensitizer can interacts with different substrates to form free radicals. These radicals can also interact with oxygen producing ROS. In the type II partway, the photosensitizer generates singlet molecular oxygen, $O_2(^1\Delta_g)$, by energy transfer [7].

Therefore, the development of novel photosensitizer is important to improve the efficacy of PDI. A large number of potential photosensitizers have been proposed for different microorganism [5]. In particular, 4,4-difluoro-4-bora-3a,4a-diaza-*s*-indacene (BODIPY) have attracted considerable attention due to their interesting physicochemical and spectral properties, including high absorption coefficient, fluorescence quantum yield and good photochemical stability. Several BODIPYs have to be modified to depress fluorescence and enhance singlet-to-triplet intersystem crossing for photodynamic therapy [8–10]. BODIPYs containing one pyridinium cationic group and two iodine atoms at the dipyrrolylmethene structure were able to eradicate *Staphylococcus xylosus* and *E. coli* [11]. Moreover, BODIPY substituted by *N*-methyl-4-pyridyl group was demonstrated to be efficient against planktonic and biofilms of *Pseudomonas aeruginosa* [11]. This photosensitizer exhibited antiviral, antibacterial and antifungal photoinactivation [12]. Two conjugates of a zinc(II)-dipicolylamine targeting unit and a BODIPY chromophore were studied in four bacterial strains [13]. One probe was a microbial targeted fluorescent imaging agent and the other was an oxygen photosensitizing analogue. A high fluorescence intensity of BODIPY for diagnostic imaging and an efficient antimicrobial activity may be an interesting combination. Therefore, modifications of BODIPY structures are necessary to optimize the phototoxicity efficacies.

In this work, two cationic BODIPY derivatives, **3** and **4** (Scheme 1), were synthetized from the condensation of the corresponding pyrrole and benzaldehyde, follow by complexation with boron and methylation with methyl iodide. The development of cationic amphiphilic photosensitizers has showed several interesting applications for a variety of biological systems [14]. The positive charge on the photosensitizer molecule appear to promote a tight electrostatic interaction with negatively charged sites at the outer surface of the Gram-negative bacteria, increasing the efficiency of the photoinactivation processes [5]. Also, cationic photosensitizer can be effective to killing yeast cells [15]. The spectroscopic and photodynamic properties of these BODIPYs were studied in homogeneous media of different polarities and in a simple biomimetic system formed by reverse micelles. 1,3-Diphenylisobenzofuran (DPBF) was used to sense $O_2(^1\Delta_g)$ formation, while the amino acid L-tryptophan (Trp) was investigated as possible molecular target of ROS in a cellular environment. Moreover, the effect of addition of the inert inorganic salt potassium iodide (KI) was studied in the decomposition of substrates. Preliminary studies of photodynamic inactivation were performed using typical microorganisms, a Gram-positive bacterium *S. aureus*, a Gram-negative bacterium *E. coli* and a yeast *C. albicans*.

2. Materials and methods

2.1. General

Proton nuclear magnetic resonance spectra were performed on a FT-NMR Bruker Avance DPX400 spectrometer at 400 MHz. Mass Spectra were recorded on a Bruker micrO-TOF-QII (Bruker Daltonics, MA, USA) equipped with an atmospheric pressure photoionization (APPI) source. Absorption spectra were carried out on a Shimadzu UV-2401PC spectrometer (Shimadzu Corporation, Tokyo, Japan). Cell growth was measured with a Turner SP-830 spectrophotometer (Dubuque, IA, USA). Fluorescence spectra were performed on a Spex FluoroMax spectrofluorometer (Horiba Jobin Yvon Inc, Edison, NJ, USA). Fluence rates were obtained with a Radiometer Laser Mate-Q (Coherent, Santa Clara, CA, USA). Photooxidation of substrates were carried out with a Cole-Parmer illuminator 41720-series (Cole-Parmer, Vernon Hills, IL, USA) with a 150 W halogen lamp through a high intensity grating monochromator (Photon Technology Instrument, Birmingham, NJ, USA) with a fluence rate of 0.74 mW/cm^2 at 500 nm. The visible light source used to irradiate cell suspensions was a Novamat 130 AF (Braun Photo Technik, Nürnberg, Germany) slide projector containing with a 150 W lamp. A 2.5 cm glass cuvette filled with water was used to remove the heat from the lamp. A wavelength range between 350 and 800 nm was selected by optical filters with a fluence rate of 70 mW/cm^2 at 500 nm. Chemicals from Aldrich (Milwaukee, WI, USA) were used without further purification. Sodium bis(2-ethylhexyl)sulfosuccinate (AOT) from Sigma (St. Louis, MO, USA) was dried under vacuum. Silica gel thin-layer chromatography (TLC) plates 250 μm from Analtech (Newark, DE, USA) were used.

2.2. Synthesis of BODIPYs

1,3,5,7-Tetramethyl-8-[4-(*N*,*N*-dimethylamino)phenyl]-4,4-difluoro-4-bora-3*a*,4*a*-diaza-*s*-indacene **1**. A solution of 2,4-dimethylpyrrole (620 μL, 6.02 mmol), 4-(*N*,*N*-dimethylamino) benzaldehyde (450 mg, 3.02 mmol) and trifluoroacetic acid (TFA, 50 μL, 0.65 mmol) in 150 mL of CH_2Cl_2 was stirred overnight under an argon atmosphere at room temperature. TLC analysis showed a relevant consumption of the aldehyde. After that, 2,3-dichloro-5,6-dicyano-1,4-benzoquinone (DDQ, 681 mg, 3.00 mmol) in 50 mL of CH_2Cl_2 was dropped in the reaction flask and the mixture was stirred for an additional 20 min. Then, an excess of trimethylamine (TEA, 9 mL, 64.6 mmol) and boron trifluoride diethyl etherate ($BF_3{\cdot}OEt_2$, 9 mL, 72.9) were added and the reaction mixture was

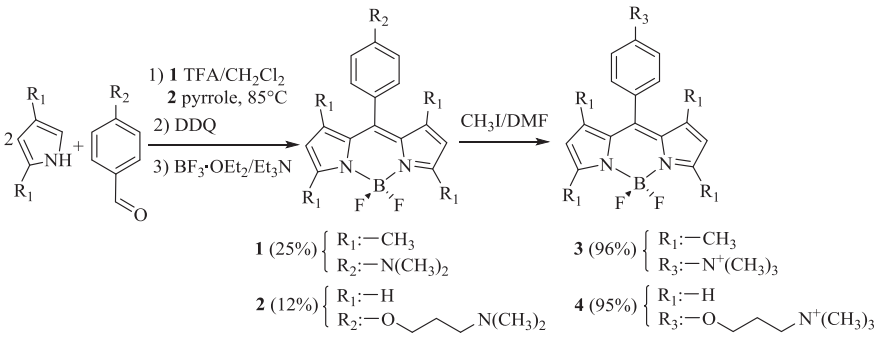

Scheme 1. Synthesis of BODIPYs **1**–**4**.

stirred for 12 h. The organic layer containing the crude product was washed with water and the organic solution was dried over Na_2SO_4. The solvent was evaporated under reduced pressure. Flash column chromatography (silica gel) using CH_2Cl_2 as eluent afforded 275 mg (25%) of BODIPY **1** as orange needles. TLC (CH_2Cl_2) $R_f = 0.60$. ^{1}HNMR ($CDCl_3$, TMS) δ [ppm] 1.48 (s, 6H), 2.55 (s, 6H), 3.04 (s, 6H, -N(CH_3)$_2$), 5.97 (s, 2H, pyrrole), 6.82 (d, 2H, $J = 8.7$ Hz, Ar), 7.08 (d, 2H, $J = 8.7$ Hz, Ar). APPI-MS [m/z] 368.2110 $(M + H)^+$ (367.2031 calculated for $C_{21}H_{24}BF_2N_3$).

8-[4-(3-(*N*,*N*-Dimethylamino)propoxy)phenyl]-4,4-difluoro-4-bora-3*a*,4*a*-diaza-*s*-indacene **2**. A solution of 4-[3-(*N*,*N*-dimethylamino)propoxy]benzaldehyde (2 mL, 9.95 mmol) and pyrrole (15.0 mL, 216.2 mmol) was treated as previously described to obtain 1.77 g (55%) of *meso*-[4-(3-*N*,*N*-dimethylaminopropoxy) phenyl]dipyrromethane [16]. A mixture of this dipyrromethane (829 mg, 2.57 mmol) and DDQ (1.06 g, 4.67 mmol) in 130 mL of CH_2Cl_2 was stirred for 3 h at room temperature. Then, TEA (12 mL, 86.1 mmol) and $BF_3{\cdot}OEt_2$ (12 mL, 97.2 mmol) were added. The mixture was stirred for an additional 12 h at room temperature and then was washed with water for two times (10 mL each). The solvent was evaporated under reduced pressure. Flash column chromatography (silica gel, CH_2Cl_2/Et_3N 1%) yielded 114 mg (12%) of pure BODIPY **2**. TLC (CH_2Cl_2/Et_3N 1%) $R_f = 0.74$. ^{1}HNMR ($CDCl_3$, TMS) δ [ppm] 1.96 (m, 2H), 2.30 (s, 6H, -N(CH_3)$_3$), 2.67 (t, 2H, $J = 6.0$ Hz), 4.11 (t, 2H, $J = 6.1$ Hz), 6.55 (dd, 2H, $J = 1.7$, 4.2 Hz, pyrrole), 6.97 (d, 2H, $J = 4.2$ Hz, pyrrole), 7.04 (d, 2H, $J = 8.3$ Hz, Ar), 7.53 (d, 2H, $J = 8.3$ Hz, Ar), 7.92 (br, 2H, pyrrole). APPI-MS [m/z] 370.1902 $(M + H)^+$ (369.1824 calculated for $C_{20}H_{22}BF_2N_3O$).

1,3,5,7-Tetramethyl-8-[4-(*N*,*N*,*N*-trimethylamino)phenyl]-4,4-difluoro-4-bora-3*a*,4*a*-diaza-*s*-indacene **3**. A mixture of BODIPY **1** (20 mg, 0.052 mmol) and methyl iodide (200 μL, 3.21 mmol) in 2 mL of *N*,*N*-dimethylformamide (DMF) was stirred for 72 h at 40 °C. The solvents were removed under vacuum to obtain 25 mg (96%) of BODIPY **3**. ^{1}HNMR (DMSO-d_6, TMS) δ [ppm] 1.53 (s, 6H), 2.46 (s, 6H), 3.66 (s, 9H, -N(CH_3)$_3$), 6.21 (s, 2H, pyrrole), 7.71 (d, 2H, $J = 8.8$ Hz, Ar), 8.14 (d, 2H, $J = 8.8$ Hz, Ar). APPI-MS [m/z] 383.2344 $(M + H)^+$ (382.2261 calculated for $C_{22}H_{27}BF_2N_3$).

8-[4-(3-(*N*,*N*,*N*-Trimethylamino)propoxy)phenyl]-4,4-difluoro-4-bora-3*a*,4*a*-diaza-*s*-indacene **4**. A mixture of BODIPY **2** (10 mg, 0.027 mmol) and methyl iodide (200 μL, 3.21 mmL) in 2 mL of DMF was stirred for 72 h at 40 °C. The solvents were removed under vacuum to yield 15 mg (95%) of BODIPY **4**. ^{1}HNMR (DMSO-d_6, TMS) δ [ppm] 2.18 (m, 2H), 3.04 (s, 9H, -N(CH_3)$_3$), 3.37 (t, 2H, $J = 6.2$ Hz), 4.17 (t, 2H, $J = 6.0$ Hz), 6.69 (dd, 2H, $J = 1.8$, 4.2 Hz, pyrrole), 7.02 (d, 2H, $J = 4.2$ Hz, pyrrole), 7.17 (d, 2H, $J = 8.3$ Hz, Ar), 7.66 (d, 2H, $J = 8.3$ Hz, Ar), 8.09 (br, 2H, pyrrole). APPI-MS [m/z] 441.2763 $(M + H)^+$ (440.2679 calculated for $C_{25}H_{33}BF_2N_3O$).

2.3. Spectroscopic studies

UV-visible absorption and fluorescence spectra of BODIPYs (3.4 μM) were recorded in a quartz cell of 1 cm path length at 25.0 ± 0.5 °C. Reverse micelles of *n*-heptane/AOT (0.1 M)/water ($W_0 = 10$) were prepared as previously described [17]. The steady-state fluorescence emission spectra were performed exciting the samples at $\lambda_{exc} = 470$ nm. Absorbances (<0.05) were matched at the excitation wavelength and the areas of the emission spectra were integrated in the range of 480–700 nm. The energy of the singlet-state (E_s) was calculated from the intersection of the normalized absorption and fluorescence curves. The fluorescence quantum yield (Φ_F) of BODIPYs were calculated by comparison of the area below the corrected emission spectrum with that of fluorescein as a reference ($\Phi_F = 0.92$ in 0.1 M NaOH) and taking into account the refractive index of the solvents [18]. Singlet excited state deactivation of BODIPY by KI was investigated using Stern-Volmer's Equation (1):

$$\frac{I_0}{I} = 1 + k_q\tau^0[Q] = 1 + K_{SV}[Q] \quad (1)$$

where I_0 and I are the fluorescence intensity of BODIPY in the absence and in the presence of quencher, k_q represents the biomolecule quenching rate constant, τ^0 the excited state lifetime of BODIPY in the absence of KI, [Q] is the KI concentration and K_{SV} is the Stern-Volmer quenching constants.

2.4. Photooxidation of DPBF

Solutions of DPBF (20 μM) and BODIPY in DMF or *n*-heptane/AOT (0.1 M)/water ($W_0 = 10$) media were irradiated in 1 cm path length quartz cells (2 mL) with monochromatic light at $\lambda_{irr} = 500$ nm (BODIPY absorbance 0.1). The kinetics of DPBF photooxidation were studied following the decrease of the absorbance (A) at $\lambda_{max} = 413$ nm. The observed rate constants (k_{obs}) were obtained by a linear least-squares fit of the semilogarithmic plot of Ln A_0/A *vs.* time. Values of quantum yields of $O_2(^1\Delta_g)$ production (Φ_Δ) in DMF were calculated comparing the k_{obs} for the corresponding BODIPY with that for C_{60}, which was used as a reference ($\Phi_\Delta = 1$) [19]. Measurements of the sample and reference under the same conditions afforded Φ_Δ for photosensitizers by direct comparison of the slopes in the linear region of the plots. Also, photooxidation of DPBF by BODIPYs was evaluated in the presence of different concentrations of KI (10 and 50 mM) in DMF/5% water.

2.5. Photooxidation of Trp

Solutions of Trp (20 μM) and BODIPY in DMF were treated as described above for photodecomposition of DPBF. Photooxidation of Trp was studied by exciting the samples at $\lambda_{exc} = 290$ nm and following the decrease of the fluorescence intensity at $\lambda = 341$ nm. Control experiments showed that under these conditions the fluorescence intensity correlates linearly with Trp concentration. The observed rate constants (k_{obs}) were obtained by a linear least-squares fit of semi-logarithmic plots of ln (I_0/I) *vs.* time. Similarly, photooxidation of Trp was performed in presence of IK (50 mM) in DMF/10% water. Also, decomposition of Trp by BODIPYs in DMF/10% water was investigated by adding diazabicyclo[2.2.2]octane (DABCO, 50 mM) and D-mannitol (50 mM).

2.6. Generation of iodine species

UV-visible spectra of the solution containing BODIPY (1 μM) and 10 mM of KI in DMF/5% water was performed before and after irradiation with visible light at different times (5, 10, 15 and 30 min) under aerobic condition. Also, the same experiment was carried out in an argon atmosphere. Diluted Lugol's solution (20 μM) was used to obtain reference spectra in DMF/5% water. Also, a control was performed irradiating KI in absence of the BODIPYs.

2.7. Photosensitized inactivation of microorganisms

The microorganisms used in this study were the strains of *S. aureus* ATCC 25923, *E. coli* (EC7) and *C. albicans* (PC31), which were previously characterized and identified [20]. Microbial cell suspensions (2 mL, ~10^8 colony forming units (CFU)/mL bacteria and ~10^6 CFU/mL yeast) in 10 mM phosphate-buffered saline (PBS, pH = 7.4) solution were incubated with 50 mM KI for 10 min in dark at 37 °C. After that, cells were treated with BODIPY **3** or **4** (1 μM for *S. aureus* and 5 μM for *E. coli* and *C. albicans*) for 30 min in dark at 37 °C in Pyrex culture tubes (13 × 100 mm). KI were added from a

stock solution (1 M) in water and photosensitizer from a stock solution (~0.5 mM) in DMF. Then, 200 μL of each cell suspension were transferred to 96-well microtiter plates (Deltalab, Barcelona, Spain). Cells were exposed to visible light for 5 min (*S. aureus*), 15 min (*E. coli*) and 30 min (*C. albicans*). The number of viable cells was determined as previously described [20].

2.8. Controls and statistical analysis

Control experiments were performed in presence and absence of photosensitizer in the dark and in the absence of photosensitizer with cells irradiated. The amount of DMF (<1% v/v) used in each experiment was not toxic to microbial cells. Three values were obtained per each condition and each experiment was repeated separately three times. The unpaired *t*-test was used to establish the significance of differences between groups. Differences between means were tested for significance by one-way ANOVA. Results were considered statistically significant with a confidence level of 95% ($p < 0.05$). Data were represented as the mean ± standard deviation of each group.

3. Results

3.1. Synthesis of BODIPYs

The synthetic procedures to obtain BODIPYs are summarized in Scheme 1. BODIPY **1** was synthesized from 4-(*N*,*N*-dimethylamino) benzaldehyde and 2,4-dimethylpyrrole catalyzed by TFA in CH_2Cl_2. BODIPY **2** was obtained from 4-[3-(*N*,*N*-dimethylamino)propoxy] benzaldehyde and a large excess of pyrrole. The mixture was heated to 85 °C and catalyst was not added. The dipyrromethane-forming reaction also can be performed at elevated temperature in the absence of acid [16]. Under these reaction conditions, pyrrole serves as the reactant in excess and as the solvent for the reaction, giving the direct formation of *meso*-[4-(3-*N*,*N*-dimethylaminopropoxy)phenyl]dipyrromethane. The dipyrromethanes were aromatized with DDQ resulting in a dipyrromethene that is ultimately converted to the BODIPY by complexation with a difluoroboryl unit in a base-catalyzed reaction with boron trifluoride diethyl etherate, using TEA [21]. Flash chromatography on silica gel yielded 25% and 12% of the product **1** and **2**, respectively. Iodine substitution of BODIPYs **1** and **2** was tested with I_2/HIO_3 using the conditions previously reported [22]. However, in the presence of (*N*,*N*-demethylamino)phenyl and (*N*,*N*-dimethylamino)propoxyphenyl groups on the *meso* position of the BODIPY skeleton, iodination also occurs on the aromatic ring. This undesired reaction cannot be avoid due to these electron donor groups promote electrophilic aromatic substitution, which occurs on the phenyl contemporaneously with the iodination of the 2,6 free positions. Also, electrophilic iodination produces polysubstitution on the diaza-*s*-indacene ring of BODIPY **2**. Therefore, this approach produces multiple products with low yields.

The amine groups in the structure of BODIPYs **1** and **2** were the precursors of cationic BODIPYs **3** and **4** by methylation. Thus, cationic BODIPYs were obtained by treating **1** and **2** with an excess of methyl iodide (Scheme 1). The exhaustive methylation produced BODIPYs **3** and **4** in 96% and 95% yields, respectively.

3.2. Absorption and fluorescence spectroscopic properties of BODIPYs

The absorption spectra of the BODIPYs **3** and **4** in different media are shown in Fig. 1. The main absorption band of both BODIYs is centered about 500 nm in the pure solvents. The spectroscopic properties of these BODIPYs are compiled in Table 1. This

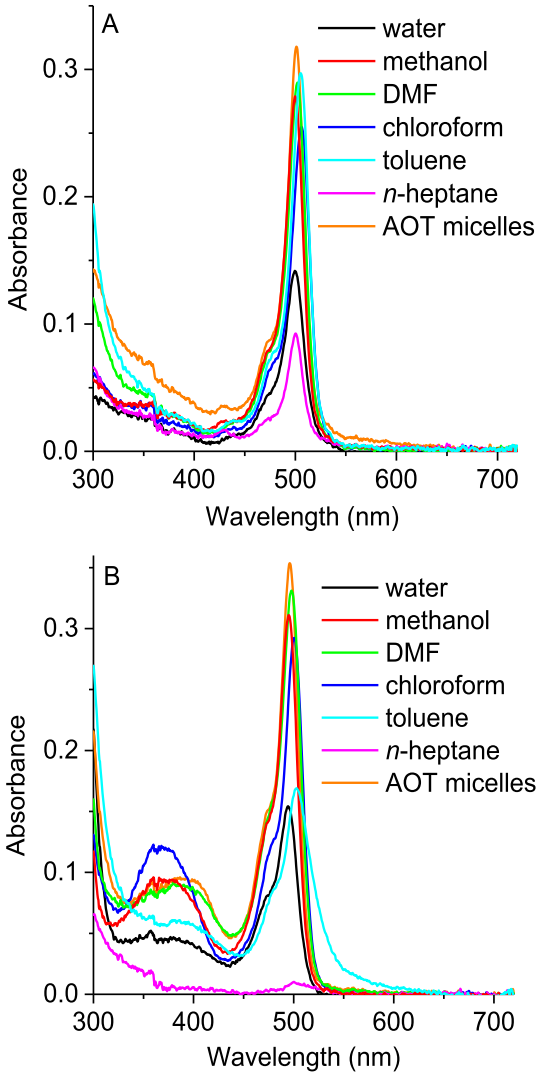

Fig. 1. Absorption spectra of BODIPYs (A) **3** and (B) **4** in different solvents and AOT micelles; *n*-heptane/AOT (0.1 M)/water ($W_0 = 10$); [BODIPY] = 3.4 μM.

Table 1
Spectroscopic properties of BODIPYs **3** and **4** in DMF.

Parameters	Media	**3**	**4**
λ_{max}^{Abs} (nm)[a]	DMF	502	498
ε ($M^{-1}cm^{-1}$)	DMF	8.51×10^4	9.49×10^4
λ_{max}^{Em} (nm)[a]	DMF	513	512
E_s (eV)	DMF	2.44	2.45
Φ_F	DMF	0.29 ± 0.02	0.030 ± 0.005

[a] [BODIPY] = 3.4 μM.

band was attributed to the 0-0 vibrational band of a strong $S_0 \rightarrow S_1$ transitions [23,24]. A shoulder at the short wavelength side can be observed centered at approximately 475 nm, which is assigned to the 0–1 vibrational band of the same transition. Moreover, the transition band $S_0 \rightarrow S_2$ at ~370 nm was observed for BODIPY **4**. The position of the $S_0 \rightarrow S_1$ absorption band shows minor solvent-dependent shifts, indicating a weak charge transfer character for the lowest electronic excitation in the ground-state geometry. Sharp absorption bands were obtained for both BODIPYs in methanol, DMF and chloroform, indicating that the photosensitizers are mainly non-aggregated in these solvents (Fig. 1). A small

hypsochromic effect (5 nm for **3** and 8 nm for **4**) in the maximum of band was produced in more polar solvents respect to non-polar media, such as methanol with respect to toluene. At the concentration tested (3.4 μM), both BODIPYs are dissolved in water showing the characteristic absorption band at ~500 nm. On the other hand, BODIPY **4** is poorly soluble in *n*-heptane, evidenced by the low absorption, possibly due to the polarity of the amino group in the aliphatic chain. Therefore, the solubilization of these cationic BODIPYs were spectroscopically analyzed in *n*-heptane/AOT (0.1 M)/water (W_0 = 10) reverse micelles. When the absorption spectra of BODIPY **3** were studied in AOT micelles, an increase in the intensity and a small hypsochromic effect of 4 nm in the maximum of the band was observed respect to *n*-heptane. Also, the absorbance of BODIPY **4** increase in AOT micelles with respect to *n*-heptane. The spectrum of BODIPYs in this microheterogenic system was very similar to that in DMF (Fig. 1). Thus, both BODIPYs were dissolved as monomer in the micellar system.

Fluorescence emission spectra of these BODIPYs were compared in DMF (Fig. 2). The bands around 512 nm are characteristic for similar BODIPYs [25]. These bands have been assigned to the 0-0 vibrational band of the $S_1 \rightarrow S_0$ transitions [18]. The energy levels of the singlet excited state (E_s) were calculated taking into account the energy of the 0-0 electronic transitions (Table 1). The values of E_s are similar to those previously reported for this kind of BODIPYs [26,27]. From the difference between positions of the band maxima of the absorption and emission spectra of the 0-0 electronic transition, Stokes shifts of 11 and 14 nm were calculated for BODIPYs **3** and **4**, respectively. Fluorescence quantum yields (Φ_F) of these compounds were calculated in DMF (Table 1). The value of Φ_F for BODIPY **3** agrees with previously reported for similar BODIPYs [25,28]. In contrast, BODIPY **4** showed only very weak emission as was found for this kind of compounds [29].

3.3. Photosensitized decomposition of DPBF

The photooxidation of DPBF induced by BODIPYs was first studied in DMF. DPBF can be decomposed by $O_2(^1\Delta_g)$ to produce 1,2-dibenzoylbenzene [30]. Thus, this substrate was used to evaluate the ability of the BODIPYs to produce $O_2(^1\Delta_g)$. After irradiation, the formation of products interfering in the absorption spectra was not detected. Also, the absorption due to BODIPYs was unchanged, indicating no significant photobleaching in this period. Therefore, the decrease in absorption of DPBF can be assigned to the photooxidation of this substrate mediated by BODIPYs. A time-dependent decrease in the DPBF concentration was observed by following its absorbance at 413 nm (Fig. 3A). From first-order kinetic plots the values of the observed rate constant (k_{obs}) were calculate for DPBF. The results are shown in Table 2. Moreover, the values of Φ_Δ were calculated comparing the slope for BODIPYs **3** and **4** with the corresponding slope obtained for the reference, C_{60}. These BODIPYs photodecompose DPBF with lower rates than C_{60}, indicating that $O_2(^1\Delta_g)$ was poorly produced in this medium. Also, photodecomposition of DPBF photosensitized by BODIPY **3** was higher than that of BODIPY **4**.

Moreover, photooxidation of DPBF mediated by BODIPYs **3** and **4** was investigated in *n*-heptane/AOT (0.1 M)/water (W_0 = 10) reverse micelles under aerobic conditions (Fig. 3B). Photodecomposition of DPBF by $O_2(^1\Delta_g)$ takes place in the toluene pseudophase where this non-polar molecule is mainly solubilized. As shown in Table 2, a higher reaction rate of DPBF photooxidation was found for BODIPYs **3** and **4** in the AOT system than in DMF.

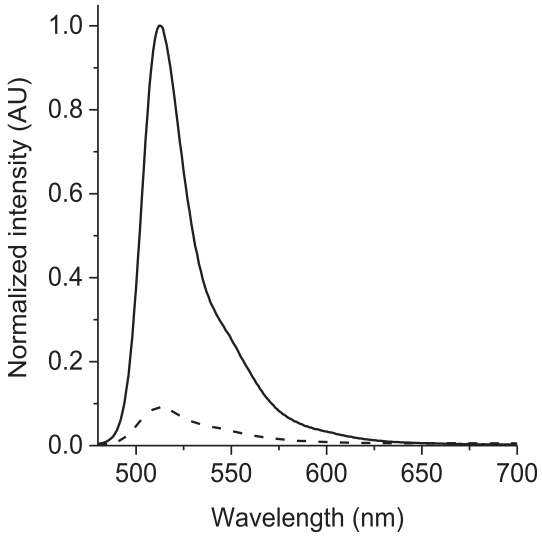

Fig. 2. Fluorescence emission spectra of BODIPYs **3** (solid line) and **4** (dashed line) in DMF, λ_{exc} = 470 nm.

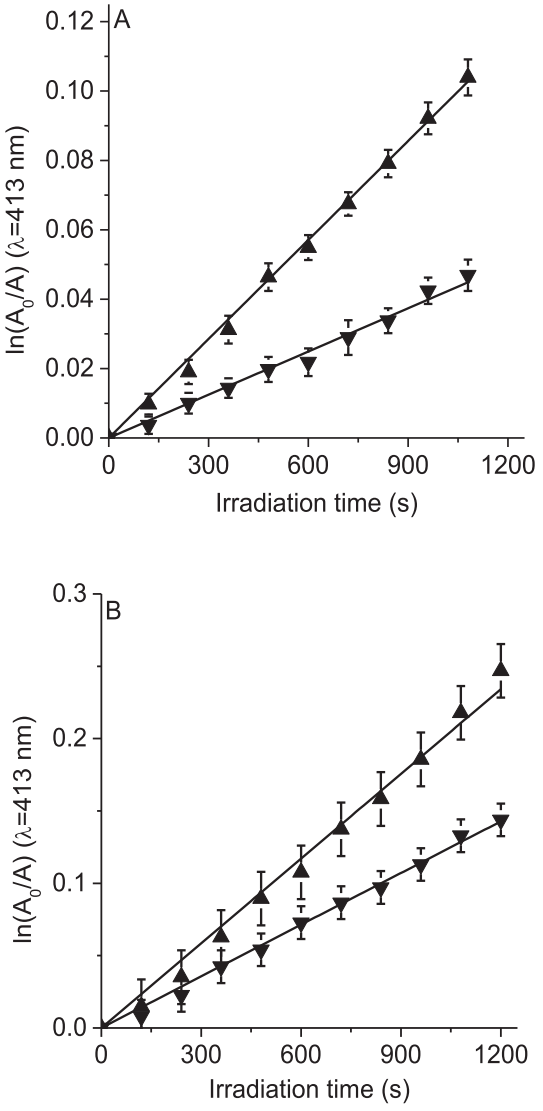

Fig. 3. First-order plots for the photooxidation of DPBF (20 μM) photosensitized by **3** (▲) and **4** (▼) in (A) DMF and (B) *n*-heptane/AOT (0.1 M)/water (W_0 = 10), λ_{irr} = 500 nm.

Table 2
Kinetic parameters for the photooxidation reaction of DPBF (k_{obs}^{DPBF}) and Trp (k_{obs}^{Trp}) and $O_2(^1\Delta_g)$ quantum yield (Φ_Δ).

Parameters	Media	**3**	**4**
k_{obs}^{DPBF} (s^{-1})	DMF	$(9.51 \pm 0.05) \times 10^{-5}$	$(4.15 \pm 0.03) \times 10^{-5}$
Φ_Δ[a]	DMF	0.07 ± 0.01	0.03 ± 0.01
k_{obs}^{DPBF} (s^{-1})	AOT micelles[b]	$(1.95 \pm 0.03) \times 10^{-4}$	$(1.25 \pm 0.02) \times 10^{-4}$
k_{obs}^{Trp} (s^{-1})	DMF	$(3.06 \pm 0.02) \times 10^{-4}$	$(3.44 \pm 0.02) \times 10^{-4}$
k_{obs}^{Trp} (s^{-1})	DMF/5% water	$(4.75 \pm 0.05) \times 10^{-5}$	$(7.86 \pm 0.07) \times 10^{-5}$
$k_{obs}^{Trp+DABCO}$ (s^{-1})[c]	DMF/5% water	$(2.98 \pm 0.06) \times 10^{-5}$	$(3.00 \pm 0.02) \times 10^{-5}$
$k_{obs}^{Trp+mannitol}$ (s^{-1})[d]	DMF/5% water	$(1.41 \pm 0.05) \times 10^{-5}$	$(1.56 \pm 0.03) \times 10^{-5}$

[a] Reference fullerene C_{60}, $k_{obs}^{DBPF}=(1.44 \pm 0.03) \times 10^{-3}$ s^{-1}, $\Phi_\Delta = 1$.
[b] *n*-heptane/AOT (0.1 M)/water ($W_0 = 10$).
[c] 50 mM DABCO.
[d] 50 mM D-mannitol.

3.4. Photooxidation of Trp

Photosensitized decomposition of Trp by BODIPYs **3** and **4** was investigated in DMF. As shown in Fig. 4, the photooxidation followed first-order kinetics with respect to Trp concentration. From these plots, the values of the k_{obs}^{Trp} were determined for Trp decomposition. The results are summarized in Table 2. As can be observed, high photooxidation rates of Trp were obtained using these BODIPYs as photosensitizers. In contrast to that observed with DPBF, a higher reaction rate of Trp photooxidation was found using BODIPY **4** than BODIPY **3**.

3.5. Effect of scavengers of ROS on the photooxidation of Trp

The effect of suppressors of ROS, DABCO and D-mannitol, were investigated to obtain insight about the photodynamic mechanism involved in the photosensitized oxidation of Trp mediated by BODIPYs **3** and **4**. The reaction was studied in DMF/5% water because the additives were added from a stock solution in water. First-order plots for the photooxidation of Trp are shown in Fig. 5. In this media, the reaction rate of Trp mediated by both BODIPYs was slower than in DMF (Table 2). This effect may be influenced by a shorter lifetime of $O_2(^1\Delta_g)$ in the polar medium containing water with respect to pure DMF [31].

To evaluate the possible involvement of $O_2(^1\Delta_g)$, experiments were performed in presence of 50 mM DABCO. A charge transfer-induced mechanism was suggested for the quenching of $O_2(^1\Delta_g)$ by DABCO [32]. This compound was used to inhibit $O_2(^1\Delta_g)$-mediated oxidations and to suppress $O_2(^1\Delta_g)$-sensitized fluorescence.

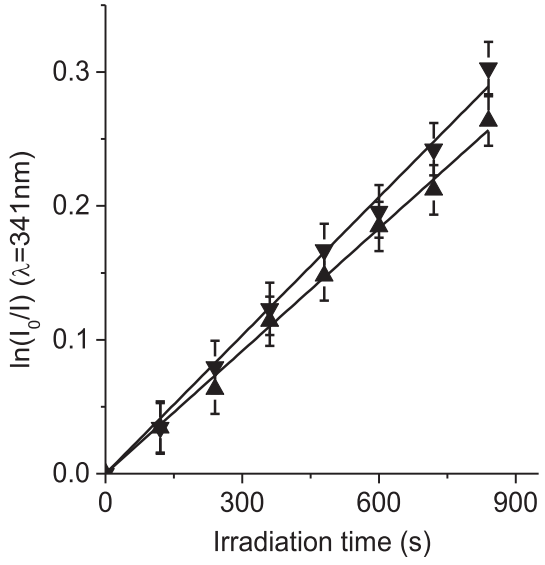

Fig. 4. First-order plots for the photooxidation of Trp (20 μM) photosensitized by **3** (▲) and **4** (▼) in DMF, $\lambda_{irr} = 500$ nm.

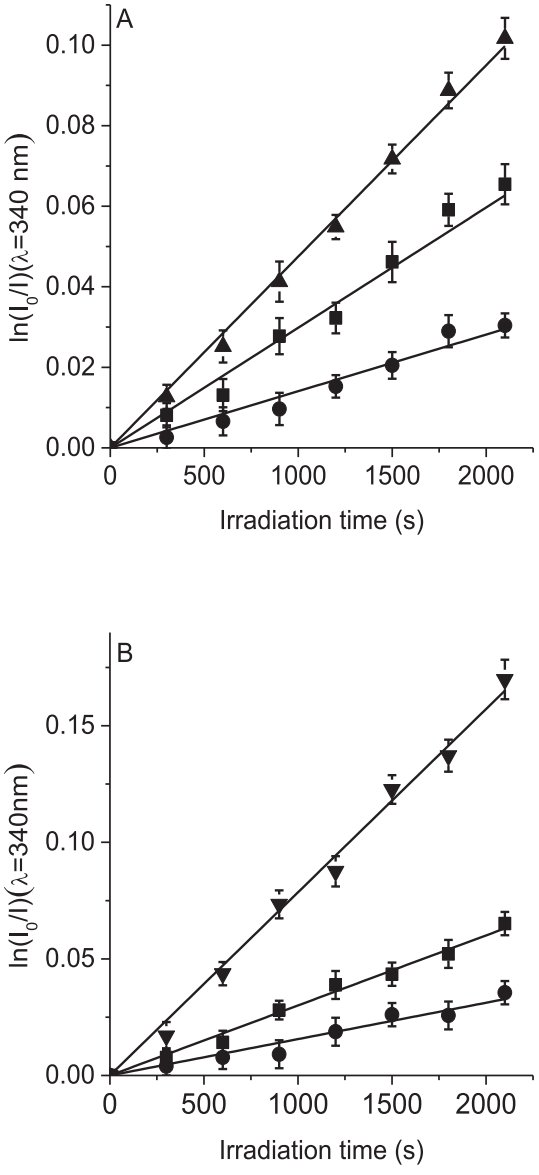

Fig. 5. First-order plots for the photooxidation of Trp (20 μM) in DMF/5% water photosensitized by: (A) **3** (▲) and (B) **4** (▼) with addition of DABCO (50 mM) (●) and D-mannitol (50 mM) (■), $\lambda_{irr} = 500$ nm.

For both BODIPYs, the values of k_{obs} (Table 2) decreased in presence of DABCO. On the other hand, the photooxidation of Trp was investigated in presence of 50 mM D-mannitol. This compound can be used as a scavenger of the superoxide anion radical ($O_2^{\bullet -}$) and hydroxyl radical (HO•) (type I reaction) [33]. Fig. 5 shows the Trp decomposition mediated by BODIPYs in solutions containing D-mannitol. For both BODIPYs, the reaction rate of Trp was diminished due to the photoprotective effect produced by D-mannitol (Table 2).

3.6. Effect of KI on fluorescence emission

The effect of KI on the fluorescence spectrum of BODIPYs **3** and **4** was investigated in DMF/10% water. The values of Φ_F were calculated at different KI concentrations (Table 3). The fluorescence efficiency of BODIPYs was diminished with increasing amounts of the quencher. This is confirmed by the Stern-Volmer plot shown in Fig. 6. The slope of this line corresponds to the quenching constant, K_{SV}. The values obtained for quenching of fluorescence by iodide ions are summarized in Table 3. A higher K_{SV} value was obtained for BODIPY **3** than **4**.

3.7. Effect of KI on the photooxidation of DPBF

Photooxidation of DPBF sensitized by BODIPYs **3** and **4** was investigated varying KI concentrations in DMF/5% water. As shown in Fig. 7, the photooxidation followed first-order kinetics with respect to DPBF concentration. From the plots in Fig. 7, the values of the k_{obs}^{DPBF} were calculated for DPBF decomposition. The results shown in Table 4 indicate a higher value of k_{obs} for the reaction in absence of KI. For both BODIPYs, the reaction rate diminished in presence of KI. The effect of iodine ions was more pronounced for reaction sensitized by BODIPY **4**. In presence of 50 mM KI, the k_{obs} value decreased by a factor of 1.8 for BODIPY **3**, while it was 9.0 for BODIPY **4**.

3.8. Effect of KI on the photooxidation of Trp

When Trp photooxidation was studied varying KI concentration in DMF/5% water, the disappearance of the amino acid following the behavior showed in Fig. 8. A value of k_{obs}^{Trp} higher was obtained for the reaction sensitized by BODIPY **4** with respect to **3** (Table 4). The value k_{obs}^{Trp} diminished with increasing the amount of water in the medium. However, the addition of 50 mM KI produced an increase in the reaction rates of Trp decomposition. The effect of KI was greater for the photoprocess sensitized by BODIPY **4**, which produces more than three times increase in the reaction rate.

3.9. Iodine generation

To verify the generation of iodine in the system, the spectra of solutions with BODIPY and BODIPY + KI (10 mM) were performed after different irradiation times (5, 10, 15 and 30 min) with visible light (Fig. 9). The formation of iodine species was evaluated by measuring the peak at 360 nm [34]. Also, it was compared with positive control of diluted Lugol's solutions. As shown in Fig. 9, we observed the production of iodine species when the samples were irradiated for different times. In contrast, no peak was found in the spectra of the solutions without photosensitizer irradiated for 30 min or with photosensitizer in dark. Moreover, solutions containing BODIPY **3** or **4** and KI were irradiated for 30 min under an argon atmosphere no changes were observed in the spectra in comparison with the dark control.

Table 3
Quenching of BODIPYs fluorescence emission by KI in DMF/5% water.

Parameters	[KI] (mM)[a]	3	4
Φ_F	0	0.29 ± 0.02	0.030 ± 0.001
	10	0.25 ± 0.01	0.029 ± 0.001
	25	0.18 ± 0.01	0.026 ± 0.001
	50	0.13 ± 0.02	0.024 ± 0.001
K_{SV} (M^{-1})	–	51.8 ± 0.6	13.0 ± 0.4

[a] [BODIPY] = 3.4 μM.

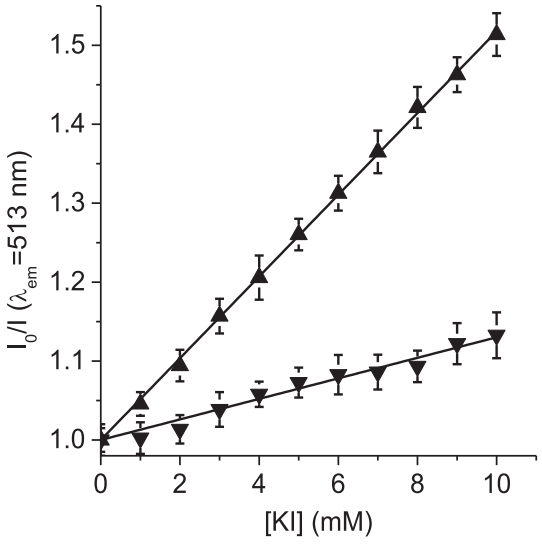

Fig. 6. Variation of fluorescence emission intensity of **3** (▲) and **4** (▼) as a function of KI concentrations in DMF, λ_{exc} = 470 nm, λ_{em} = 513 nm.

3.10. Photosensitized inactivation of microorganisms

Photosensitized inactivation of *S. aureus*, *E. coli* and *C. albicans* was investigated in PBS cell suspensions (Fig. 10). *S aureus* was incubated with 1 μM photosensitizer, while *E. coli* and *C. albicans* were treated with 5 μM photosensitizer. The viability of the microbial cells was not affected by irradiation without photosensitizer nor to cells treated with photosensitizer in the dark. Also, cell survival was not modified by the presence of 50 mM KI (results no shown). After 5 min irradiation, both BODIPYs produced a reduction >5 log in the cell survival of *S. aureus* (Fig. 10A). In presence of 50 mM KI, a slight increase (~0.5 log) was observed in the photoinactivation of this Gram-positive strain. In *E. coli*, these BODIPYs induced a ~2.5 log decrease in cell survival after 15 min irradiation (Fig. 10B). The effect of KI produced an increase of 1.0 log in the photoinactivation sensitized by BODIPY **3**, while BODIPY **4** achieved a practically complete eradication. In yeast, the photodynamic activity of BODIPY **3** yielded a 3.7 log decrease in the *C. albicans* cell viability after 30 min irradiation (Fig. 10C). In contrast, BODIPY **4** induced a 0.9 log reduction in the survival of the yeast. The addition of KI produced an enhanced photoinactivation of 1.1 log and 3.5 log for BODIPY **3** and **4**, respectively.

4. Discussion

The presence of amine groups in the phenylene bonded to position 8 of the diaza-*s*-indacene ring can modulate the amphiphilic character of the compounds by forming cationic substituents. This allows increasing the solubility of BODIPYs in the biological environment, enhancing the binding and penetration into the cell membranes. The mainly difference between both cationic BODIPYs

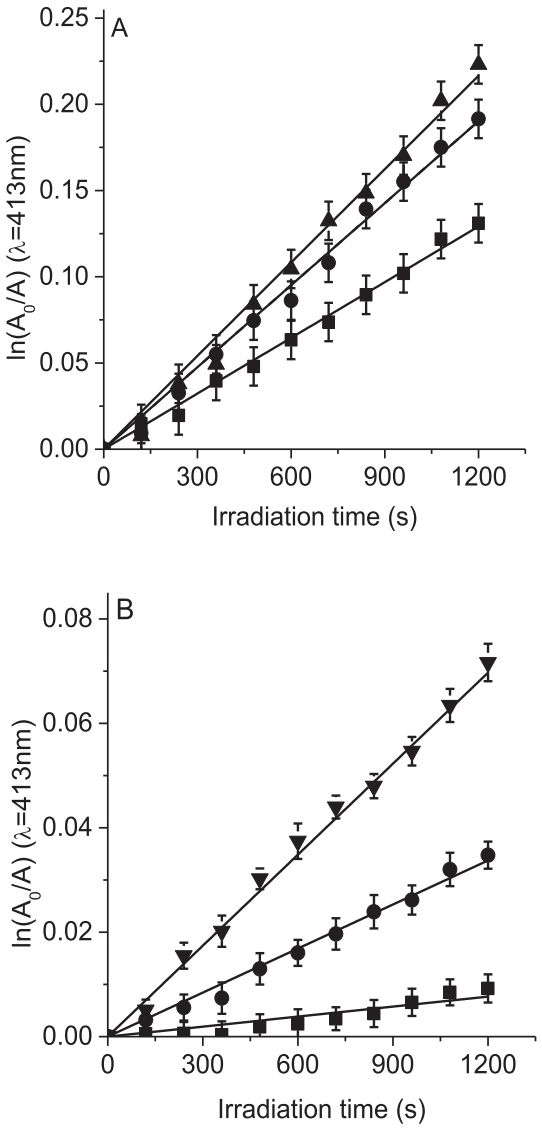

Fig. 7. First-order plots for the photooxidation of DPBF (20 μM) in DMF/5% water photosensitized by (A) **3** (▲), **3** with addition of 10 mM KI (●) and 50 mM KI (■). (B) **4** (▼), **4** with addition of 10 mM IK (●) and 50 mM KI (■), λ_{irr} = 500 nm.

3 and **4** is the presence of an aliphatic quaternary ammonium cation group in BODIPY **4**. In this structure the cationic center is isolated from the BODIPY by a propoxy bridge. Thus, this charge has minimal influence on the electronic density of the BODIPY. This helps to retain the consistency of the photophysical properties of the BODIPY. Also, this chain provides a higher mobility of the charge, which could facilitate the interaction with the cell envelope of microorganisms [16]. Another important difference is the β-substitution by methyl groups in BODIPY **3**, which influence the rotation of the *meso*-phenyl ring [29].

Both compounds exhibited typical spectral characteristics of the BODIPY core with a narrow absorption band at ~500 nm and high molar extinction coefficients (~10^5 M^{-1} cm^{-1}). Substitution at the *meso* position of the BODIPY core did not significantly alter the absorption bands that are observed in this kind of compounds without substitution [35]. The spectra were also studied in *n*-heptane/AOT (0.1 M)/water (W_0 = 10) reverse micelles. This microheterogeneous media have been used as a simple model to mimic the water pockets often found in various bioaggregates [36,37]. Depending on the polarity, a photosensitizer can be located in the organic surrounded solvent, the water pool or at the micellar AOT interface. The spectroscopic studies indicate that the BODIPYs **3** and **4** are not aggregated in the micelles. Moreover, both BODIPYs showed hyperchromic shift in AOT system respect to *n*-heptane. This effect can be attributed to the interaction between the BODIPYs and the AOT micelles, indicating that these photosensitizers are associated with the micellar interface [38].

The absorption and emission spectra were almost mirror images of each other, indicating that the emitting and absorbing species are similar. Small Stokes shifts indicated that in these molecules the spectroscopic energies are similar to the relaxed energies of the lowest singlet excited state S_1, according to the rigid planar structure of the BODIPYs [26]. This suggests that only a minor geometric relaxation occurs in the first excited state. The value of Φ_F for BODIPY **3** agrees with that previously reported for 1,3,5,7-tetramethyl-8-[4-(*N*,*N*-dimethylamino)phenyl]-4,4-difluoro-4-bora-3*a*,4*a*-diaza-*s*-indacene upon protonation of the aniline nitrogen in TFA/methanol [28]. This value is appropriated for quantification of photosensitizers by fluorescence emission techniques in biological media [17]. However, fluorescence emission of BODIPY **4** was about one order of magnitude less than BODIPY **3** in DMF. Similar results were previously obtained for 5-substituted borondipyrrin dyes, which were only weakly fluorescent, in contrast to the intense fluorescence of the analogous β-substituted dipyrrin based dye [18]. The low fluorescence was assigned to the free rotation of the *meso*-substituents [39]. The β-substitution in BODIPY **3** prevents the free rotation of the *meso*-phenyl group, and reduced the number of nonradiative decay pathways in this structure. Therefore, the structural change in BODIPY **4** has an important effect on the photophysical properties of the S_1 state [29]. The rotation of the phenylene ring distorts the dipyrrin backbone and thereby promotes nonradiative decay of the excited state. The much lower fluorescence quantum yield of BODIPY **4** indicates an enhanced rate of internal conversion ($S_1 \rightarrow S_0$) due to rapid rotation of the mesophenyl ring in the unhindered molecule. Therefore, it is important to note this behavior, which crucially affects the performance of fluorescence, for designing molecular structures in order to use them as fluorophores for imaging techniques. On the other hand, BODIPY **4** can be an interesting structure for study in fluorescence anisotropy techniques for imaging in cells. It can be used to sense changes in viscosity in the biological environment, by increasing its emission in environments more viscous, due to the reduction or prevention of the rotation of the substituent group [40]. Also, it was previously found that for BODIPY **1** the fluorescence was quenched at neutral or basic pH due to

Table 4
Kinetic parameters for the photooxidation reaction of DPBF (k_{obs}^{DPBF}) and Trp (k_{obs}^{Trp}) in presence of different additives.

Parameters	Media	Additive	**3**	**4**
k_{obs}^{DPBF} (s^{-1})	DMF/5% water	–	$(1.80 \pm 0.03) \times 10^{-4}$	$(5.81 \pm 0.04) \times 10^{-5}$
	DMF/5% water	10 mM KI	$(1.58 \pm 0.02) \times 10^{-4}$	$(2.79 \pm 0.03) \times 10^{-5}$
	DMF/5% water	50 mM KI	$(1.02 \pm 0.01) \times 10^{-4}$	$(0.64 \pm 0.05) \times 10^{-5}$
k_{obs}^{Trp} (s^{-1})	DMF/10% water	–	$(2.13 \pm 0.03) \times 10^{-5}$	$(2.79 \pm 0.04) \times 10^{-5}$
	DMF/10% water	50 mM KI	$(4.42 \pm 0.06) \times 10^{-5}$	$(9.55 \pm 0.05) \times 10^{-5}$

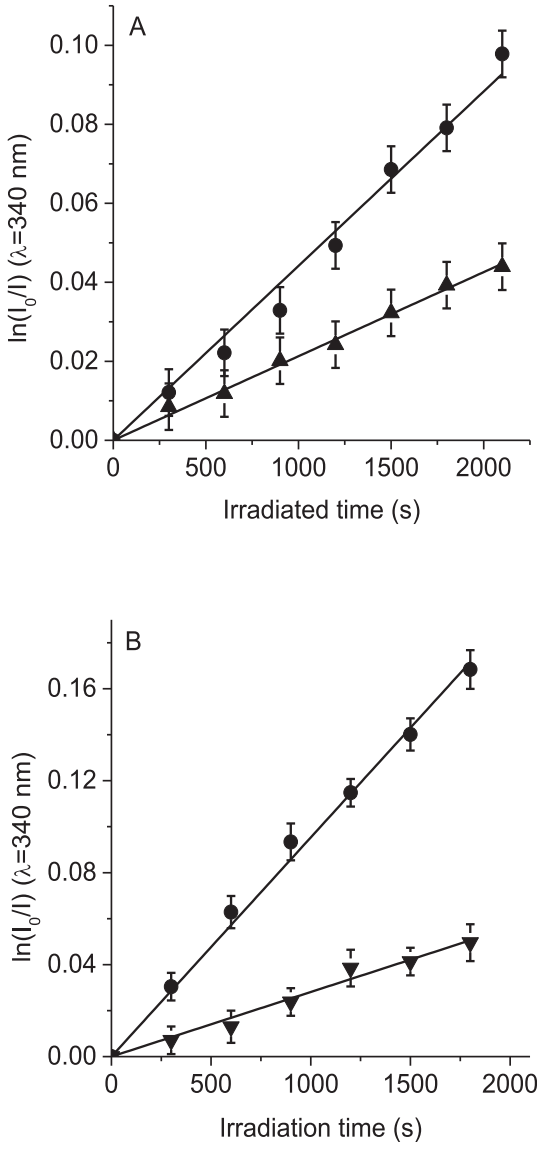

Fig. 8. First-order plots for the photooxidation of Trp (20 μM) in DMF/10% water photosensitized by (A) **3** (▲) and (B) **4** (▼) without addition and with addition of KI (50 mM) (●), λ_{irr} = 500 nm.

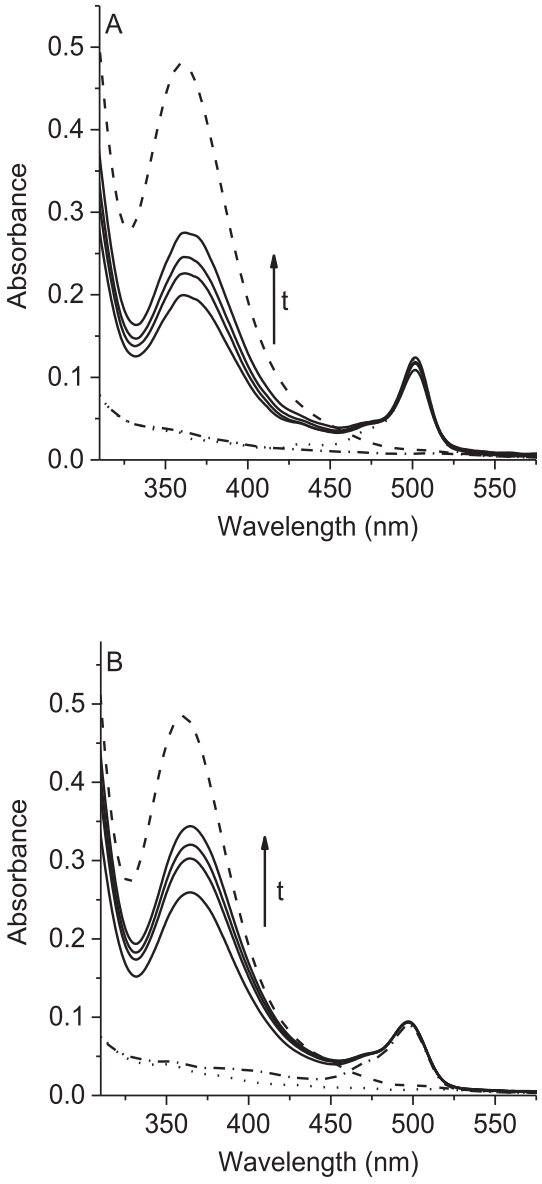

Fig. 9. Absorption spectra of the solution containing (A) **3** and (B) **4** in DMF/5% water and 10 mM KI after different irradiation times (5, 10, 15 and 30 min, solid lines) with visible light. As control was used the spectra obtained from the Lugol's solution (20 μM, dashed line), solution without photosensitizer irradiated for 30 min (dotted line) and solution with photosensitizer in dark (dotted and dashed line).

photoinduced electron transfer (PeT) [28]. However, upon protonation of the aniline nitrogen fluorescence intensity increases drastically. A similar effect was observed in BODIPY **3** because the methylation of amine group also avoids PeT.

A low generation of $O_2(^1\Delta_g)$ photosensitized by BODIPYs **3** and **4** was found in DMF. Similar results of $O_2(^1\Delta_g)$ production were previously found for 1,3,5,7-tetramethyl-8-(substituted phenyl)-4,4′-difluoroboradiazaindacene using DPBF in isopropanol [22,41]. Moreover, photosensitized oxidation of DPBF by 8-phenyl-4,4′-difluoroboradiazaindacene was not detected in either polar or nonpolar solvents [42]. The direct measurements of $O_2(^1\Delta_g)$ revealed that photogeneration of this reactive oxygen species by the structurally related BODIPY derivatives was very low in acetonitrile [43]. Moreover, photooxidation of DPBF was compared in AOT micelles. In this system, compounds of different polarities can be dissolved simultaneously. Decomposition of DPBF by $O_2(^1\Delta_g)$ was faster than in DMF. In general, photooxidation of substrates by $O_2(^1\Delta_g)$ are slower in AOT reverse micelles due to the partition of $O_2(^1\Delta_g)$ between the internal and external pseudophases [37,44]. However, these BODIPYs can interact with the AOT micelles through their cationic substituents. These compounds can locate at the micellar interface because their amphiphilic character. Localization of BODIPYs in the micellar interface decrease the vibrational decay, favoring the photosensitization of $O_2(^1\Delta_g)$ from the BODIPY triplet state. Therefore, photooxidation DPBF sensitized by BODIPYs was faster in this microheterogenic organized system than DMF.

BODIPYs **3** and **4** were able to produce a rapid photooxidation of Trp in DMF. It is known that Trp can be photooxidized by both type I and type II reaction mechanisms [45,46]. Proteins comprise a majority of the dry weight of a cell, rendering them a major target for oxidative modification [47]. Decomposition of Trp residues in proteins specifically can have effects detrimental to the health of cells. Therefore, this amino acid can be a potential target of the ROS generated by BODIPYs in cells. From the kinetic results of Trp and DPBF in DMF under the same conditions, it can be calculated that

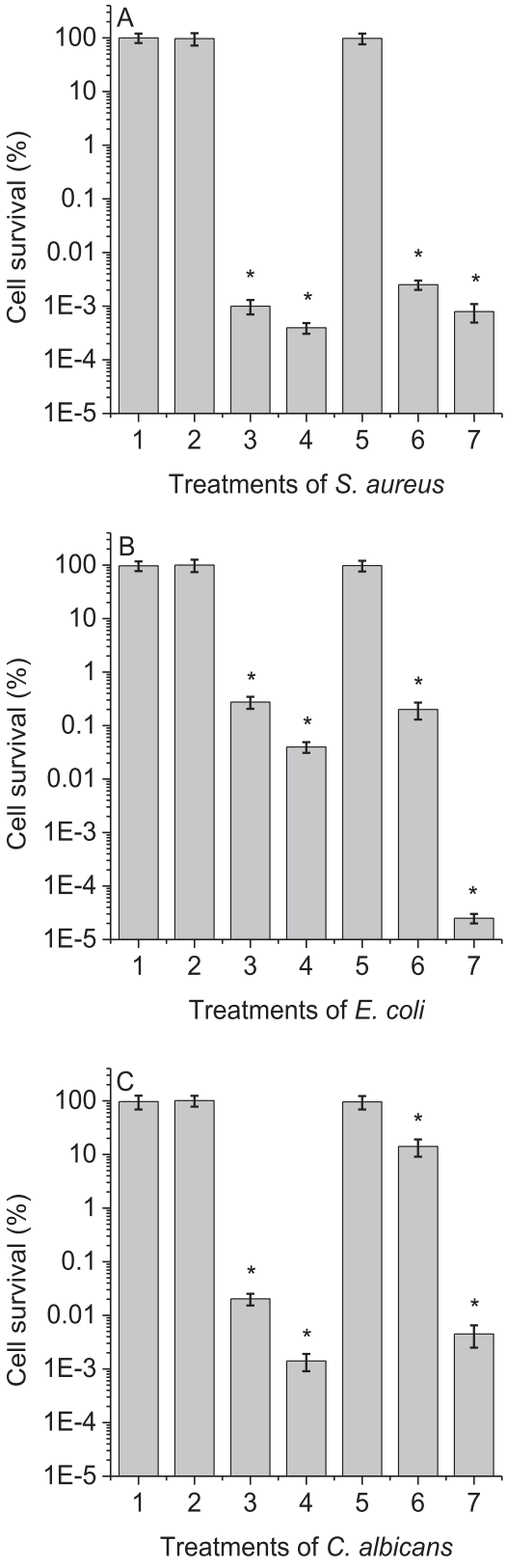

Fig. 10. Survival of (A) *S. aureus* (~10^8 CFU/mL) treated with 1 μM photosensitizer, (B) *E. coli* (~10^8 CFU/mL) treated with 5 μM photosensitizer and (C) *C. albicans* (~10^6 CFU/mL) treated with 5 μM photosensitizer and irradiated with visible light for 5, 15 and 30 min, respectively; 1) irradiated cells without photosensitizer; 2) cells treated with **3** in dark; 3) irradiated cells treated with **3**; 4) irradiates cells treated with 50 mM KI and **3**; 5) cells treated with **4** in dark; 6) irradiated cells treated with **4**; 7) irradiated cells treated with 50 mM KI and **4** (*$p < 0.05$, compared with control).

the ratio $k_{obs}^{Trp}/k_{obs}^{DPBF}$ takes values of 3.2 and 8.3 for BODIPYs **3** and **4**, respectively. On the other hand, taking into account the second-order rate constant of Trp and DPBF with $O_2(^1\Delta_g)$ a ration of k_r^{Trp}/k_r^{DPBF} of about 0.07 can be calculated, which is considerably lower than the values of $k_{obs}^{Trp}/k_{obs}^{DPBF}$ found with BODIPYs [31]. Therefore, a type I pathway may be also contributing, together with type II photoprocess, to Trp decomposition in DMF [44]. This effect is more pronounced using BODIPY **4**, which has isolated the cationic group by an aliphatic chain avoiding interaction with the main structure of the indacene ring. The involvement of both photodynamic mechanisms was confirmed by the addition of DABCO and D-mannitol. Photooxidation of Trp decreased in presence of DABCO, indicating the intermediacy of $O_2(^1\Delta_g)$ [32]. Also, D-mannitol produced a reduction in the decomposition of Trp, which is expected when a type I process is involved in the reaction of the amino acid [33]. Therefore, photooxidation of Trp showed a significant contribution of type I mechanism in the photodecomposition of the biological substrate by BODIPYs. In previous studies using BODIPYs, with similar structures and characteristics, was also found the participation of type I mechanism in the generation of ROS species, mainly the intermediacy of $O_2^{\bullet-}$ [41,48].

It was observed that emission from BODIPYs **3** and **4** was decreased using KI as a fluorescence quencher. KI is known to enhance the rate of intersystem crossing of many dyes by external heavy-atom effect [49,50]. Also, this inorganic salt was found to enhance the triplet-state decay rate by a charge-coupled deactivation [50]. Therefore, considering an increase in the intersystem crossing of BODIPYs in the presence of KI, it would be expected an increased production of $O_2(^1\Delta_g)$. In contrast, a protective effect was found for the photooxidation of DPBF, which was depended on KI concentration. It was previously observed that when added in micromolar concentrations KI can act as an antioxidant, promoting the recovery of photooxidized fluorophores [50]. In aqueous media, the reaction of iodide anions and $O_2(^1\Delta_g)$ results in the production of triiodide anions (I_3^-). In this process hydrogen peroxide (H_2O_2) is formed, which can react further with iodide anions to generate I_3^- [51,52]. On the other hand, the photooxidation of Trp considerably increased in presence of KI. The characteristic spectrum of the I_3^- was obtained after irradiation of BODIPYs solutions containing KI. However, I_3^- was not obtained in an argon atmosphere, indicating that it is formed by the reaction with $O_2(^1\Delta_g)$. In this system, unstable iodine atoms (I•) and iodine radical anions ($I_2^{\bullet-}$) can also be generated by interaction of I^- with HO• [53]. The generated I• is presumed to react with I^- to yield $I_2^{\bullet-}$ [54]. Two $I_2^{\bullet-}$ can react to form I_3^- and I^- by disproportionation [55]. Oxidative degradation of Trp can be found under different ionization condition of proteins [56]. Also, Trp seem to be competitive inhibitors of the iodide oxidation reaction, and therefore may react with the oxidized form of iodide [57]. It was proposed that the interaction of the ROS and KI during light exposure, biocidal molecular iodine (I_2) or I_3^- can be formed improving bacterial inactivation [53]. In the present study, photoinactivation of *S. aureus* was slight affected by the presence of KI due to this bacterium was the most susceptible strain. An increase of microbial inactivation of *E. coli* and *C. albicans* was observed by adding KI. The effect of iodide was mainly observed for BODIPY **4**. This tendency was also found in the decomposition de Trp. Thus, the formation of reactive iodine species can be involved in the damage to microbial cell. Therefore, this complementary pathway of induced damage can be used to potentiate the photodynamic activity produced by BODIPYs in microorganisms.

5. Conclusions

Cationic BODIPYs **3** and **4** were obtained by methylation of the corresponding non-charged BODIPYs, which were synthetized by

acid-catalyzed condensation of corresponding pyrrole and benzaldehyde derivatives and complexation with boron. The two BODIPYs differ by virtue of the substitution pattern at the pyrrole units and the link of the cationic *N*,*N*,*N*-trimethylamino group to the phenylene unit. Compounds **3** and **4** showed similar absorption spectroscopic properties. However, a considerably lower fluorescence emission was found for **3** than **4**, due to the rotation of the phenylene ring that promotes nonradiative decay of the excited state. These BODIPYs showed a low production of $O_2(^1\Delta_g)$. Nevertheless, they efficiently induced the photodecomposition of Trp, possibly with a contribution of type I photoprocess. The addition of KI produced an increase in the photoinduced decomposition of Trp. Reactive iodine species can be formed by the reaction of iodide with ROS and they may be contributing to decompose Trp. Therefore, the addition of KI could be used to potentiate the photoinactivation of microorganisms sensitized by BODIPYs **3** and **4**. Further studies of photosensitization *in vitro* are presently in progress in our laboratory.

Acknowledgements

Authors are grateful to Consejo Nacional de Investigaciones Científicas y Técnicas (CONICET, PIP-2015 1122015 0100197 CO) of Argentina, SECYT Universidad Nacional de Río Cuarto (PPI-2016 18/C460) and Agencia Nacional de Promoción Científica y Tecnológica (FONCYT, PICT-2012 0714) of Argentina for financial support. E.N.D. is Scientific Member of CONICET. M.L.A., M.B.B., E.R and E.D.Q. thank to CONICET for the research fellowships.

References

[1] A. Nigama, D. Gupta, A. Sharma, Treatment of infectious disease: beyond antibiotics, Microbiol. Res. 169 (2014) 643–651.
[2] U. Theuretzbacher, Global antibacterial resistance: the never-ending story, J. Glob. Antimicrob. Resist 1 (2013) 63–69.
[3] G. Criseo, F. Scordino, O. Romeo, Current methods for identifying clinically important cryptic Candida species, J. Microbiol. Methods 111 (2015) 50–56.
[4] D.M.A. Vera, M.H. Haynes, A.R. Ball, T. Dai, C. Astrakas, M.J. Kelso, M.R. Hamblin, G.P. Tegos, Strategies to potentiate antimicrobial photoinactivation by overcoming resistant phenotypes, Photochem. Photobiol. 88 (2012) 499–511.
[5] E. Alves, M.A. Faustino, M.G. Neves, A. Cunha, J. Tome, A. Almeida, An insight on bacterial cellular targets of photodynamic inactivation, Fut. Med. Chem. 6 (2014) 141–164.
[6] T.G.St. Denis, T. Dai, L. Izikson, C. Astrakas, R.R. Anderson, M.R. Hamblin, G.P. Tegos, All you need is light: antimicrobial photoinactivation as an evolving and emerging discovery strategy against infectious disease, Virulence 2 (2011) 509–520.
[7] P.R. Ogilby, Singlet oxygen: there is still something new under the sun, and it is better than ever, Photochem. Photobiol. Sci. 9 (2010) 1543–1560.
[8] S.G. Awuah, Y. You, Boron dipyrromethene (BODIPY)-based photosensitizers for photodynamic therapy, RSC Adv. 2 (2012) 11169–11183.
[9] A. Kamkaew, S.H. Lim, H.B. Lee, L.V. Kiew, L.Y. Chung, K. Burgess, BODIPY dyes in photodynamic therapy, Chem. Soc. Rev. 42 (2013) 77–88.
[10] J. Zhao, K. Xu, W. Yang, Z. Wang, F. Zhong, The triplet excited state of Bodipy: formation, modulation and application, Chem. Soc. Rev. 44 (2015) 8904–8939.
[11] E. Caruso, S. Banfi, P. Barbieri, B. Leva, V.T. Orlandi, Synthesis and antibacterial activity of novel cationic BODIPY photosensitizers, J. Photochem. Photobiol. B Biol. 114 (2012) 44–51.
[12] B.L. Carpenter, X. Situ, F. Scholle, J. Bartelmess, W.W. Weare, R.A. Ghiladi, Antiviral, antifungal and antibacterial activities of a BODIPY-based photosensitizer, Molecules 20 (2015) 10604–10621.
[13] D.R. Rice, H. Gan, B.D. Smith, Bacterial imaging and photodynamic inactivation using zinc(II)-dipicolylamine BODIPY conjugates, Photochem. Photobiol. Sci. 14 (2015) 1271–1281.
[14] H. Abrahamse, M.R. Hamblin, New photosensitizers for photodynamic therapy, Biochem. J. 473 (2016) 347–364.
[15] P. Calzavara-Pinton, M.T. Rossi, R. Sala, M. Venturini, Photodynamic antifungal chemotherapy, Photochem. Photobiol. 88 (2012) 512–522.
[16] D.A. Caminos, E.N. Durantini, Synthesis of asymmetrically *meso*-substituted porphyrins bearing amino groups as potential cationic photodynamic agents, J. Porphyr. Phthalocyanine 9 (2005) 334–342.
[17] M. Novaira, M.P. Cormick, E.N. Durantini, Spectroscopic and time-resolved fluorescence emission properties of a cationic and an anionic porphyrin in biomimetic media and *Candida albicans* cells, J. Photochem. Photobiol. A Chem. 246 (2012) 67–74.
[18] H.L. Kee, C. Kirmaier, L. Yu, P. Thamyongkit, W.J. Youngblood, M.E. Calder, L. Ramos, B.C. Noll, D.F. Bocian, W.R. Scheidt, R.R. Birge, J.S. Lindsey, D. Holten, Structural control of the photodynamics of boron-dipyrrin complexes, J. Phys. Chem. B 109 (2005) 20433–20443.
[19] R. Hung, J. Grabowski, A precise determination of the triplet energy of C_{60} by photoacoustic calorimetry, J. Phys. Chem. 95 (1991) 6073–6075.
[20] D.D. Ferreyra, E. Reynoso, P. Cordero, M.B. Spesia, M.G. Alvarez, M.E. Milanesio, E.N. Durantini, Synthesis and properties of 5,10,15,20-tetrakis [4-(3-*N*,*N*-dimethylaminopropoxy)phenyl]chlorin as potential broad-spectrum antimicrobial photosensitizers, J. Photochem. Photobiol. B Biol. 158 (2016) 243–251.
[21] L.C.D. de Rezende, F. da Silva Emery, A review of the synthetic strategies for the development of BODIPY dyes for conjugation with proteins, Orbital Elec. J. Chem. 5 (2013) 62–83.
[22] S. Banfi, G. Nasini, S. Zaza, E. Caruso, Synthesis and photo-physical properties of a series of BODIPY dyes, Tetrahedron 69 (2013) 4845–4856.
[23] M. Baruah, W. Qin, C. Flors, J. Hofkens, R.A.L. Vallée, D. Beljonne, M. Van der Auweraer, W.M. De Borggraeve, N. Boens, Solvent and pH dependent fluorescent properties of a dimethylaminostyryl borondipyrromethene dye in solution, J. Phys. Chem. A 110 (2006) 5998–6009.
[24] N. Shivran, M. Tyagi, S. Mula, P. Gupta, B. Saha, B.S. Patro, S. Chattopadhyay, Syntheses and photodynamic activity of some glucose-conjugated BODIPY dyes, Eur. J. Med. Chem. 122 (2016) 352–365.
[25] J. Bartelmess, W.W. Weare, Preparation and characterization of multi-cationic BODIPYs and their synthetically versatile precursors, Dyes Pigment. 97 (2013) 1–8.
[26] A. Harriman, L.J. Mallon, G. Ulrich, R. Ziessel, Rapid intersystem crossing in closely-spaced but orthogonal molecular dyads, Chem. Phys. Chem. 8 (2007) 1207–1214.
[27] J. Zhao, W. Wu, J. Sun, S. Guo, Triplet photosensitizers: from molecular design to applications, Chem. Soc. Rev. 42 (2013) 5323–5351.
[28] S. Hoogendoorn, A.E.M. Blom, L.I. Willems, G.A. van der Marel, H.S. Overkleeft, Synthesis of pH-activatable red fluorescent BODIPY dyes with distinct functionalities, Org. Lett. 13 (2011) 5656–5659.
[29] G.J. Hedley, A. Ruseckas, A. Harriman, D.W. Samuel, Conformational effects on the dynamics of internal conversion in boron dipyrromethene dyes in solution, Angew. Chem. Int. Ed. 50 (2011) 6634–6637.
[30] A. Gomes, E. Fernandes, J.L.F.C. Lima, Fluorescence probes used for detection of reactive oxygen species, J. Biochem. Biophys. Methods 65 (2005) 45–80.
[31] F. Wilkinson, W.P. Helman, A.B. Ross, Rate constants for the decay and reactions of the lowest electronically excited singlet state of molecular oxygen in solution an expanded and revised compilation, J. Phys. Chem. Ref. Data 24 (1995) 663–1021.
[32] C. Schweitzer, R. Schmidt, Physical mechanisms of generation and deactivation of singlet oxygen, Chem. Rev. 103 (2003) 1685–1757.
[33] T. Maisch, C. Bosl, R.-M. Szeimies, N. Lehn, C. Abels, Photodynamic effects of novel XF porphyrin derivatives on prokaryotic and eukaryotic cells, Antimicrob. Agents Chemother. 49 (2005) 1542–1552.
[34] J.G. Rowley, B.H. Farnum, S. Ardo, G.J. Meyer, Iodide chemistry in dye-sensitized solar cells: making and breaking I-I bonds for solar energy conversion, J. Phys. Chem. Lett. 1 (2010) 3132–3140.
[35] A. Schmitt, B. Hinkeldey, M. Wild, G. Jung, Synthesis of the core compound of the BODIPY dye class: 4,4′-difluoro-4-bora-(3a,4a)-diaza-s-indacene, J. Fluoresc. 19 (2009) 755–758.
[36] I. Scalise, E.N. Durantini, Photodynamic effect of metallo 5-(4-carboxyphenyl)-10,15,20-tris(4-methylphenyl) porphyrins in biomimetic media, J. Photochem. Photobiol. A Chem. 162 (2004) 105–113.
[37] A.L. Ochoa, T.C. Tempesti, M.B. Spesia, M.E. Milanesio, E.N. Durantini, Synthesis and photodynamic properties of adamantylethoxy Zn(II) phthalocyanine derivatives in different media and in human red blood cells, Eur. J. Med. Chem. 50 (2012) 280–287.
[38] S.J. Mora, M.E. Milanesio, E.N. Durantini, Spectroscopic and photodynamic properties of 5,10,15,20-tetrakis[4-(3-*N*,*N*-dimethylaminopropoxy)phenyl] porphyrin and its tetracationic derivative in different media, J. Photochem. Photobiol. A Chem. 270 (2013) 75–84.
[39] M. Zhang, E. Hao, J. Zhou, C. Yu, G. Bai, F. Wang, L. Jiao, Synthesis of pyrrolyldipyrrinato BF_2 complexes by oxidative nucleophilic substitution of boron dipyrromethene with pyrrole, Org. Biomol. Chem. 10 (2012) 2139–2145.
[40] M.K. Kuimova, G. Yahioglu, J.A. Levitt, K. Suhling, Molecular rotor measures viscosity of live cells via fluorescence lifetime imaging, J. Am. Chem. Soc. 130 (2008) 6672–6673.
[41] J. Wang, Y. Hou, W. Lei, Q. Zhou, C. Li, B. Zhang, X. Wang, DNA photocleavage by a cationic BODIPY dye through both singlet oxygen and hydroxyl radical: new insight into the photodynamic mechanism of BODIPYs, Chem. Phys. Chem. 13 (2012) 1–10.
[42] X.-F. Zhang, X. Yang, Photosensitizer that selectively generates singlet oxygen in nonpolar environments: photophysical mechanism and efficiency for a covalent BODIPY dimer, J. Phys. Chem. B 117 (2013) 9050–9055.
[43] M. Laine, N.A. Barbosa, A. Kochel, B. Osiecka, G. Szewczyk, T. Sarna, P. Ziółkowski, R. Wieczorek, A. Filarowski, Synthesis, structural, spectroscopic, computational and cytotoxicstudies of BODIPY dyes, Sens. Actuators B 238 (2017) 548–555.
[44] M.L. Agazzi, M.B. Spesia, N.S. Gsponer, M.E. Milanesio, E.N. Durantini,

Synthesis, spectroscopic properties and photodynamic activity of a fulleropyrrolidine bearing a basic amino group and its dicationic analog against *Staphylococcus aureus*, J. Photochem. Photobiol. A Chem. 310 (2015) 171–179.
[45] M.J. Davies, R.J.W. Truscott, Photo-oxidation of proteins and its role in cataractogenesis, J. Photochem. Photobiol. B Biol. 63 (2001) 114–125.
[46] M. Gracanin, C.L. Hawkins, D.I. Pattison, M.J. Davies, Singlet-oxygen-mediated amino acid and protein oxidation: formation of tryptophan peroxides and decomposition products, Free Radic. Biol. Med. 47 (2009) 92–102.
[47] M. Ehrenshaft, L.J. Deterding, R.P. Mason, Tripping up Trp: modification of protein tryptophan residues by reactive oxygen species, modes of detection, and biological consequences, Free Radic. Biol. Med. 89 (2015) 220–228.
[48] X.-Z. Wang, Q.-Y. Meng, J.-J. Zhong, X.-W. Gao, T. Lei, L.-M. Zhao, Z.-J. Li, B. Chen, C.-H. Tung, L.-Z. Wu, The singlet excited state of BODIPY promoted aerobic cross-dehydrogenative-coupling reactions under visible light, Chem. Commun. 51 (2015) 11256–11259.
[49] J. Widengren, P. Schwille, Characterization of photoinduced isomerization and back-isomerization of the cyanine dye Cy5 by fluorescence correlation spectroscopy, J. Phys. Chem. A 104 (2000) 6416–6428.
[50] A. Chmyrov, T. Sandén, J. Widengren, Iodide as a fluorescence quencher and promoters-mechanisms and possible implications, J. Phys. Chem. B 114 (2010) 11282–11291.
[51] J. Mosinger, M. Janošková, K. Lang, P. Kubát, Light-induced aggregation of cationic porphyrins, J. Photochem. Photobiol. A Chem. 181 (2006) 283–289.
[52] A. Felgenträger, T. Maisch, A. Späth, J.A. Schröderc, W. Bäumlera, Singlet oxygen generation in porphyrin-doped polymeric surface coating enables antimicrobial effects on *Staphylococcus aureus*, Phys. Chem. Chem. Phys. 16 (2014) 20598–20607.
[53] D. Vecchio, A. Gupta, L. Huang, G. Landi, P. Avci, A. Rodas, M.R. Hamblin, Bacterial photodynamic inactivation mediated by methylene blue and red light is enhanced by synergistic effect of potassium iodide, Antimicrob. Agents Chemother. 59 (2015) 5203–5212.
[54] J.M. Gardner, M. Abrahamsson, B.H. Farnum, G.J. Meyer, Visible light generation of iodine atoms and I-I bonds: sensitized I^- oxidation and I_3^- photodissociation, J. Am. Chem. Soc. 131 (2009) 16206–16214.
[55] G. Boschloo, A. Hagfeldt, Characteristics of the iodide/triiodide redox mediator in dye-sensitized solar cells, Acc. Chem. Res. 42 (2009) 1819–1826.
[56] G. Mourier, L. Moroder, A. Previero, Prevention of tryptophan oxidation during iodination of tyrosyl residues in peptides, Z. Naturforsch B 39 (1984) 101–104.
[57] D.P. Carvalho, A.C.F. Ferreira, S.M. Coelho, J.M. Moraes, M.A.S. Camacho, D. Rosenthal, Thyroid peroxidase activity is inhibited by amino acids, Braz. J. Med. Biol. Res. 33 (2000) 355–361.